Plume spreading in groundwater by stretching and folding

David C. Mays¹ and Roseanna M. Neupauer²

Received 28 October 2011; revised 11 April 2012; accepted 26 May 2012; published 3 July 2012.

[1] This paper proposes a new approach to the hydraulics of in situ groundwater remediation. In situ remediation promotes reactions between an injected treatment solution and the contaminated groundwater, but without a hydraulic mechanism to promote spreading, the laminar flows characteristic of porous media will keep the two fluids in approximately the same relative configuration as they travel through the aquifer, limiting the opportunity for reactions to occur. To address this fundamental limitation, this paper borrows a key result from the fluid mechanics literature: Spreading in laminar flows is optimized by chaotic advection. Previous studies have applied this result to groundwater remediation using the pulsed dipole model, but that model depends on reinjection of fluid, which presents a number of theoretical and practical limitations. Accordingly, this paper proposes a new conceptual model for plume spreading by chaotic advection, using an engineered sequence of extractions and injections of clean water at an array of wells, which generates plume spreading by stretching and folding the fluid interface between the injected treatment solution and the contaminated groundwater but does not require reinjection. The paper includes an overview of the analytical techniques—Poincaré sections, periodic points, stable and unstable manifolds, heteroclinic points, and Lyapunov exponents—used to demonstrate chaotic advection in the limiting case in which diffusion is negligible. Numerical simulations show that spreading by stretching and folding is complimentary to spreading resulting from aquifer heterogeneity.

Citation: Mays, D. C., and R. M. Neupauer (2012), Plume spreading in groundwater by stretching and folding, *Water Resour. Res.*, 48, W07501, doi:10.1029/2011WR011567.

1. Introduction

[2] Treatment solutions containing chemical amendments (oxidants, electron donors, or nutrients) are frequently injected into aquifers for in situ remediation of contaminated groundwater [Domenico and Schwartz, 1998], but this approach suffers from a fundamental technical problem: Contaminant degradation requires mixing of the treatment solution and the contaminated groundwater [MacDonald and Kitanidis, 1993], which is difficult because mixing in porous media is generally very poor [National Research Council, 2009]. Because flow in porous media is laminar, it lacks the turbulent eddies that generate most of the mixing in open channels and engineered reactors. As a result, in situ degradation reactions are confined to a narrow fluid interface between the injected plume of treatment solution and the contaminated groundwater [National Research Council, 2000], across which pore-scale dispersion is the rate-limiting step. This is a fundamental technical problem

[3] The literature on mixing in aquifers can be grouped into two broad categories, (1) heterogeneity effects, and (2) chaotic advection. Both groups generally conceptualize mixing as a two-step process with a transport step and a dispersion step. Under this paradigm, the term mixing is used in a restrictive sense for the dispersion step resulting from pore-scale processes and causing dilution, while the terms stirring, stretching, or spreading refer to the transport step resulting from advection, including heterogeneity effects manifested as macrodispersion, causing plumes to become more contorted but without dilution [Dentz et al., 2011; Kapoor and Gelhar, 1994a; Kitanidis, 1994; Le Borgne et al., 2010]. A common metric to quantify mixing is the local mixing factor $\nabla^T C \mathbf{D} \nabla C$, where $C(\mathbf{x}, t)$ is the scalar concentration of interest, and D is the dispersion tensor. For example, a recent review shows that three other mixing metrics are proportional to this local mixing factor: the rate of decay of concentration variance, the rate of growth of concentration entropy, and the rate of chemical reactions at high Damköhler number [Dentz et al., 2011]. The volume integral of the local mixing factor is the scalar dissipation rate, which has been used to quantify mixing not only in porous media [e.g., Le Borgne et al., 2010] but also in other branches of fluid mechanics [e.g., Pope, 2000]. In essentially all cases relevant to groundwater remediation, mixing is distinct from spreading, which can instead be quantified by the spatial moment of C(x, t) [Le Borgne et al., 2010] or

©2012. American Geophysical Union. All Rights Reserved. 0043-1397/12/2011WR011567

W07501 1 of 10

that has received considerable attention from the groundwater research community.

¹Department of Civil Engineering, University of Colorado Denver, Denver, Colorado, USA.

²Department of Civil, Environmental, and Architectural Engineering, University of Colorado Boulder, Boulder, Colorado, USA.

Corresponding author: D. C. Mays, Department of Civil Engineering, University of Colorado Denver, Campus Box 113, PO Box 173364, Denver, CO 80217-3364, USA. (david.mays@ucdenver.edu)

by the plume interface length [Zhang et al., 2009], both of which increase with time as the plume becomes more contorted. The latter metric is particularly appropriate for the limiting case in which pore-scale dispersion is neglected [Dagan, 1989, section 4.3.5; Kapoor and Gelhar, 1994b]. In particular, plumes in incompressible flows without dispersion maintain their initial concentration and volume [Dagan, 1989, section 4.3.5], so in this simplified case the plume interface length directly records the degree of spreading. The present study neglects dispersion in order to focus entirely on spreading, with the understanding that mixing (i.e., pore-scale dispersion) provides the final link required to increase chemical reaction rates and consequently the effectiveness of remediating groundwater by injecting treatment solutions.

[4] A review of the literature on mixing in aquifers highlights two key findings. In the first category of literature that discusses heterogeneity effects, the key finding is that spreading depends on the structure of the flow [Dentz and Carrera, 2005; Finn et al., 2004], consistent with the literature on turbulence [e.g., Crimaldi et al., 2008]. The structure of the flow in geologic porous media largely results from heterogeneous permeability [Dagan, 1989, section 4.3.5; Kapoor and Gelhar, 1994a, 1994b; Kitanidis, 1994; Rolle et al., 2009]. In the usual conceptual model, where flow results from an imposed hydraulic head gradient in a certain primary flow direction, background flow and heterogeneous permeability are required to generate heterogeneous velocity in the porous media. Recently, Le Borgne et al. [2010] generalized the role of heterogeneity by emphasizing that spreading depends on heterogeneous velocity, which could result from heterogeneous permeability, or from other mechanisms such as temporal fluctuations in the fluid velocity [Dentz and Carrera, 2005]. Once achieved, spreading enhances mixing through increased transverse dispersion [Cirpka, 2005; Cirpka et al., 2011]. In sum, the literature on heterogeneity effects articulates the need for spreading, and emphasizes that spreading depends on the structure of the flow, namely, heterogeneous velocity. It does not, however, provide guidance on what the structure of the flow can or should be to promote spreading. Accordingly, the present study proposes a new way to generate heterogeneous velocity, using extractions and injections at wells, that does not require background flow or heterogeneous permeability.

[5] The second category of literature, pioneered by Aref [1984] and Ottino [1989], falls under the heading of chaotic advection, which is known to optimize spreading in laminar flows [Ottino et al., 1994]. Chaotic advection exists when fluid particles exhibit sensitive dependence on initial conditions, which requires at least two-dimensional (2-D) unsteady flow or three-dimensional (3-D) steady flow [Ottino, 1989, section 4.7]. In particular, certain velocity fields are manifestations of the horseshoe map, a mathematical expression of stretching and folding that implies the presence of chaotic advection [Ottino et al., 1994]. Since chaotic advection optimizes spreading in laminar flows, and since stretching and folding can indicate chaotic advection, the key finding in this second category of literature is that stretching and folding can optimize spreading in laminar flows [Chakravarthy and Ottino, 1995; Ottino et al., 1994]. For example, in a theoretical study and analysis of data from the Borden site, Weeks and Sposito [1998] found that spreading is more effective if chaotic flow leading to both stretching and folding can be induced. Indeed, the importance of stretching and folding for spreading in laminar flows was first recognized more than a century ago by *Reynolds* [1894]. One can also grasp the importance of folding from a practical perspective, since only a certain degree of stretching can be accomplished within a bounded domain before folding becomes necessary to achieve continued stretching [*Aref*, 2002]. In the present application, the bounded domain is a finite region of an aquifer, to which it is beneficial to constrain remediation activity for reasons of waste containment.

[6] There are several conceptual models for chaotic advection in laminar flows, e.g., (1) the blinking vortex [Aref, 1984], (2) eccentric cylinders [Funakoshi, 2008; Muzzio et al., 1992; Swanson and Ottino, 1990], and (3) the pulsed dipole [Jones and Aref, 1988; Sposito, 2006; Stremler et al., 2004; Tel et al., 2000] and similar approaches [Bagtzoglou and Oates, 2007; Trefry et al., 2012]. Of these, the pulsed dipole merits special attention because it has found several applications, including spreading in porous media, since its introduction by Jones and Aref [1988]. Tel et al. [2000] applied the pulsed dipole to 2-D open flows, and investigated the effects of chaotic advection on chemical and biological processes in such flows. Stremler et al. [2004] investigated chaotic advection with a single pulsed dipole and with two pulsed dipoles, with applications to porous media and to microfluidics. Extending the work of Jones and Aref [1988] and Stremler et al. [2004], Sposito [2006] applied the pulsed dipole in the specific context of in situ groundwater remediation.

[7] Several other authors have reported methods similar to the pulsed dipole. Bagtzoglou and Oates [2007] numerically simulated transport in groundwater due to random extraction and injection at three wells in a triangular pattern, with no net extraction of water from the aquifer. Their results showed that this oscillating well triplet led to enhanced plume spreading. In a follow-up experimental study, Zhang et al. [2009] found that the oscillating well triplet increased the plume interface length more than a nonoscillating well triplet. Trefry et al. [2012] presented the rotating dipole based on a circular array of wells around a contaminant plume, of which two wells on opposite sides of the circle form a dipole at any given time. When the wells are operated such that the dipole pair proceeds around the circle, Trefry et al. [2012] showed the system to exhibit chaotic advection, leading to enhanced plume spreading.

[8] Although it has been applied to chaotic advection in porous media, the pulsed dipole [Jones and Aref, 1988; Sposito, 2006; Stremler et al., 2004; Tel et al., 2000] includes assumptions about the timing and orientation of reinjection of fluid particles that are not physically realistic in groundwater applications, where the timing and orientation of reinjection is random because of turbulent mixing of fluid particles in the pumps and because of dispersion in the piping between wells. Chaotic advection cannot be achieved in the pulsed dipole unless certain reinjection rules are used; in particular, Radabaugh [2011] showed a lack of chaotic advection, and hence poor spreading, on a single pass from the injection to the extraction well. Accordingly the unrealistic reinjection rules in the pulsed dipole are particularly problematic in the context of groundwater remediation. Moreover, reinjection is a regulatory concern, because

injecting contaminated water into an aquifer is generally forbidden, even in the context of groundwater remediation.

[9] The pulsed dipole also suffers from a practical limitation in groundwater applications. Because the pulsed dipole extracts both the treatment solution and the contaminated groundwater simultaneously, they will undergo turbulent mixing in the pumps, leading to reactions in the wells, rather than spatially extensive reactions throughout the aquifer itself. Such reactions near wells frequently generate clogging [Bagtzoglou and Oates, 2007; Li et al., 2009, 2010; MacDonald et al., 1999], leading to difficulty in well operations and uncertainty in the structure of the flow field. For this reason, a method that can produce spreading while minimizing plume extraction would be preferable.

[10] The goal of the present paper is to present a new approach to the hydraulics of plume spreading in the context of in situ groundwater remediation, using an engineered sequence of extractions and injections of clean water at an array of wells surrounding the injected plume of treatment solution. This engineered sequence of injections and extractions generates plume spreading by stretching and folding the fluid interface between an injected treatment solution and contaminated groundwater. The paper begins with an overview of the analytical techniques—Poincaré sections, periodic points, stable and unstable manifolds, heteroclinic points, and Lyapunov exponents—used to analyze chaotic advection. These analytical techniques are used to demonstrate chaotic advection in the engineered sequence of injections and extractions for the idealized case of homogeneous permeability. Numerical simulations are then presented to show the relative contribution of spreading resulting from stretching and folding compared to spreading resulting from aquifer heterogeneity.

2. Analytical Techniques

[11] This section provides a brief overview of the analytical techniques used to characterize chaotic advection, which will be applied to the engineered sequence of extractions and injections. This brief overview does not attempt a comprehensive treatment of these techniques, for which more complete details appear in many monographs on dynamical systems, such as those by *Ottino* [1989] and *Tabor* [1989].

2.1. Poincaré Sections

[12] In the context of periodic flows, a Poincaré section is a stroboscopic picture showing fluid particle positions at discrete time intervals [Ottino, 1989, section 5.5]. Because they help to visualize and distinguish chaotic and nonchaotic behavior, Poincaré sections are a standard technique for analyzing chaotic advection. In the present paper, the discrete time step is chosen to be the duration of the periodic pumping pattern used to drive the flow. Rather than analyzing the flow in continuous time, Poincaré sections simplify the analysis by considering the flow as an iterated map, where the map determines the coordinates for each fluid particle after each iteration of the periodic flow. Notably, in the case of potential flow, such as flow through homogeneous porous media, a Poincaré section is equivalent to a phase space plot, which is a standard tool in the literature on dynamical systems [Aref, 2002; Sposito, 2006].

2.2. Periodic Points

[13] A periodic point of period n is a point in the flow domain to which particles return exactly after n iterations of the periodic flow [e.g., Tabor, 1989]. Period n periodic points always occur in groups of size n, and can be plotted on Poincaré sections. As discussed below, periodic points are the basis for several diagnostics for chaotic advection, so their identification is a prerequisite for what follows. Periodic points can be categorized as elliptic or hyperbolic on the basis of the eigenvalues of the Jacobian that maps the periodic point back to itself. In the neighborhood of elliptic periodic points, defined by imaginary eigenvalues, spreading is poor because fluid particles become trapped inside these regions indefinitely. In the neighborhood of hyperbolic periodic points, defined by real and unique eigenvalues with one positive and one negative, spreading is good [Funakoshi, 2008; Mosovsky and Meiss, 2011], as discussed below.

2.2.1. Stable and Unstable Manifolds

[14] Spreading around hyperbolic periodic points is controlled by the stable and unstable manifolds associated with these points. A stable manifold is a curve on a Poincaré section (i.e., comprising points plotted at discrete time intervals) passing through the hyperbolic periodic point, such that particles on the stable manifold approach the periodic point in subsequent iterations of the map. An unstable manifold is similar, except that particles on the unstable manifold diverge from the hyperbolic periodic point in subsequent iterations of the periodic flow [e.g., Tabor, 1989]. A small area element on a Poincaré section in the neighborhood of the hyperbolic periodic point will be compressed along the stable manifold and stretched along the unstable manifold in such a way that its area is preserved [Tabor, 1989]. Thus, the presence of hyperbolic periodic points is characteristic of good spreading.

2.2.2. Heteroclinic Points

[15] Heteroclinic points are intersections between the stable manifold of a certain hyperbolic periodic point and the unstable manifold of a different hyperbolic periodic point. They are a significant feature because their existence implies chaos and good spreading [Ottino, 1989, section 5.9]. Moreover, the presence of one heteroclinic point implies the presence of an infinite number of heteroclinic points [Ottino, 1989, section 5.8]. Therefore heteroclinic points are a simple but compelling diagnostic for chaotic advection.

2.3. Lyapunov Exponents

[16] A fundamental aspect of chaotic advection is sensitive dependence on initial conditions, indicated by exponential growth of the separation distance of initially nearby particles. The rate of exponential growth is quantified by the Lyapunov exponent, for which the classical definition is

$$\lambda = \lim_{t \to \infty, d(0) \to 0} \left(\frac{1}{t}\right) \ln \left[\frac{d(t)}{d(0)}\right],\tag{1}$$

where d(t) is the separation distance of a pair of particles at time t [Tabor, 1989]. However, because this definition is based on the limit of long time, it is not the most appropriate metric to quantify sensitive dependence on initial

conditions in spreading applications. For example, *Swanson and Ottino* [1990] noted that a significant degree of spreading (i.e., large separation distances) is desired in the first few iterations, in contrast to generic chaotic systems, in which large separation distances are only required asymptotically (i.e., large time). Accordingly, this paper will follow the approach of *Jones and Aref* [1988], who defined a modification to the Lyapunov exponent for finite times. This paper adapts their metric as follows:

$$\lambda^{(n)} = \left(\frac{1}{n}\right) \ln \left[\frac{d(n)}{d(0)}\right],\tag{2}$$

where d(n) is the separation distance of a pair of particles after n iterations of the map. This approach is analogous to contemporary analysis of dynamical systems using finite time Lyapunov exponents [Kleinfelter et al., 2005; Stefanski et al., 2010] and related metrics [Mosovsky and Meiss, 2011].

3. Plume Spreading by Stretching and Folding

[17] This section presents a new conceptual model for plume spreading based directly on *Ottino*'s [1989, page ix] premise that spreading "is the efficient stretching and folding of material lines and surfaces."

3.1. Model Definition

[18] Consider a homogeneous, isotropic, confined, horizontal aquifer of infinite extent, porosity ε , and thickness b that

has been contaminated. To promote in situ remediation, a plume of treatment solution is injected into the contaminated aquifer, creating a circular fluid interface between the treatment solution and the contaminated groundwater, the center of which defines the point (0, 0). Degradation reactions occur where the two solutions overlap each other. To promote plume spreading, four fully penetrating wells are installed at (-L, 0), (L, 0), (0, -L) and (0, L) as shown on Figure 1a. The wells are operated in a engineered sequence of extractions and injections of clean water, with discharge Q_i and duration T_i , where i is the step number, creating a periodic, unsteady flow field within the aquifer in the vicinity of the wells. Neglecting storage effects, this is a sequence of radial flows away from the active well during injection, and toward the active well during extraction.

[19] The flow can be simulated by tracking particle positions at the end of each injection or extraction step. A volume balance around the injection well gives $Q = Aq = 2\pi rbq$, where Q > 0 is the injection rate, A is the area perpendicular to the fluid velocity, q is the specific discharge, and r is the radial distance to the active well. The fluid velocity is $v = q/\varepsilon$, where ε is porosity. Since v = dr/dt,

$$\frac{dr}{dt} = \left(\frac{Q}{2\pi b\varepsilon}\right)\frac{1}{r}.\tag{3}$$

For a fluid particle that is initially at a distance of r_o from the injection well at time t_o , (3) can be integrated from

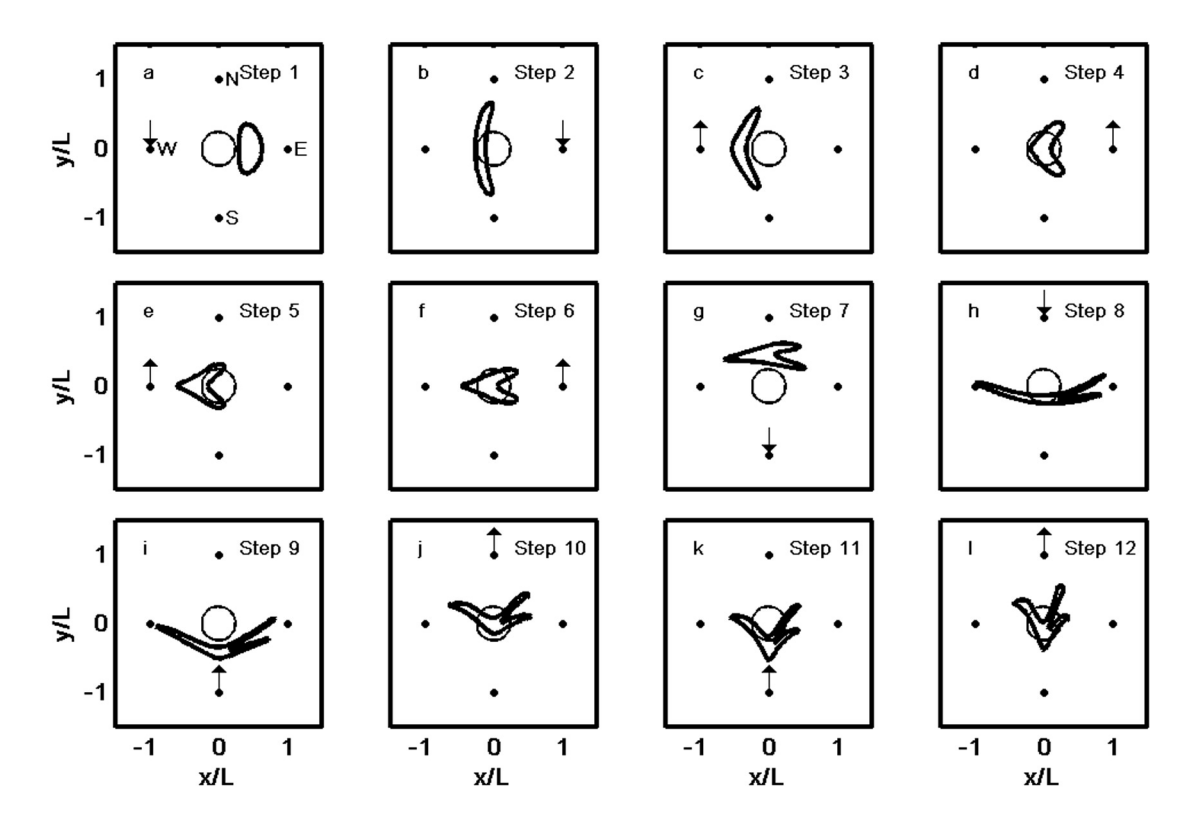


Figure 1. Plume spreading by stretching and folding using the engineered sequence of extractions and injections of Table 1. Dots denote well locations, with labels shown in Figure 1a. For reference, the initial fluid interface is shown on each plot as a thin line. Arrows denote injection (into well) or extraction (out of well).

radius r_o to r and from time t_o to t to give the radial distance from the injection well at time t,

$$r(t) = \left[\frac{Q}{\pi b \varepsilon} (t - t_o) + r_o^2\right]^{1/2}.$$
 (4)

This equation is used to calculate the position of a water particle at the end of an injection step. Since flow is radial, the particle does not move in the tangential direction. Extraction is modeled by Q < 0. The various independent variables can be grouped into a single dimensionless parameter, Λ^2 , which uniquely identifies the flow:

$$\Lambda^2 = \frac{QT}{\pi \varepsilon b L^2},\tag{5}$$

where T is the duration of injection (assumed equal to the duration of extraction) and L is the well separation distance. This expression has been generalized from *Jones and Aref* [1988] to include the effect of porosity.

[20] A sequence of extractions and injections is chosen in such a way as to create stretching and folding of the fluid interface, leading to improved spreading, and presumably therefore to enhanced reaction and more complete in situ groundwater remediation. One possible implementation of such an engineered sequence of extractions and injections is the 12-step sequence shown in Table 1 and illustrated in Figure 1 and Animation S1 of the auxiliary material. Injection or extraction rates are expressed using Λ^2 , defined in (5). The initial position of the fluid interface is assumed to be a circle of radius r = L/4 centered at the origin, giving an initial plume interface length of 1.57L. Modeling the fluid interface as a collection of particles, (4) is used to track their positions relative to the active well. In the first six steps, the west and east wells are operated. During the first two steps, water is injected, stretching the fluid interface (Figures 1a and 1b). During the next four steps, water is extracted, folding the fluid interface (Figures 1c-1f). These six steps are then repeated using the north and south wells, leading to a second fold in the fluid interface (Figures 1g–11). Equal volumes of water are injected and extracted such that the net extraction is zero. These twelve steps complete one cycle of the sequence of extractions and injections.

[21] To provide an example, if L=5 m, b=3 m, $\varepsilon=0.25$, and T=1 d, then the initial plume would have a radius of 1.25 m, the four wells would inscribe a circle of area 79 m², and the first injection rate of $\Lambda^2=+3.5/\pi$ in Table 1 would correspond to injection of 66 m³ d⁻¹ = 46 L min⁻¹.

3.2. Analysis of Chaotic Advection

[22] Analysis of the periodic points and finite time Lyapunov exponents demonstrate the presence of chaotic advection, and therefore good spreading [Aref, 1984; Ottino, 1989] in the engineered sequence of extractions and injections. Period n periodic points were identified numerically, by calculating the separation distance between the initial position and final position of a grid of particles after n cycles of extractions and injections and then finding zeros. Figure 2 shows these distances for n = 1, and Figure S1 of

Table 1. Engineered Sequence of Extractions and Injections to Stretch and Fold the Fluid Interface^a

Step	Well	Λ^2
1	W	$+3.5/\pi$
2	E	$+3.5/\pi$
3	W	$-1.0/\pi$
4	E	$-3.0/\pi$
5	W	$-1.6/\pi$
6	E	$-1.4/\pi$
7	S	$+3.5/\pi$
8	N	$+3.5/\pi$
9	S	$-1.0/\pi$
10	N	$-3.0/\pi$
11	S	$-1.6/\pi$
12	N	$-1.4/\pi$

 $^{\text{a}}\Lambda^2>0$ indicates injection.

the auxiliary material shows these distances for n=1, 2, 3, 4. In order to focus on the vicinity of the initial fluid interface, Figure 3 shows an enlargement of Figure 2 (and of Figure S1) along with corresponding results for n=2, 3, 4, with a change in color scale to emphasize small separation distances. (For comparison, Figure S2 of the auxiliary material shows Figure 3 superimposed on the position of the initially circular fluid interface, and Figure S3 repeats Figure S2 at the scale of Figure 2.) The analysis shows four period 1 periodic points (Figure 3a), four period 2 periodic points (Figure 3b), 12 period 3 periodic points (Figure 3c), and 16 period 4 periodic points (Figure 3d). Periodic points of higher period exist but are not shown in Figure 3.

[23] The classification of periodic points as elliptic or hyperbolic identifies whether the periodic points represent regions of poor spreading or good spreading, respectively. Classification of periodic points was determined by tracking a circle of 360 particles placed at a radius of r = 0.001L around each periodic point forward for 4 cycles to produce unstable manifolds, and backward for 4 cycles to produce stable manifolds (Figure 4). All period 2 periodic points and eight period 4 periodic points (shown as triangles and circles in Figures 4b and 4d) are elliptic, so the circle of particles surrounding each elliptic periodic point

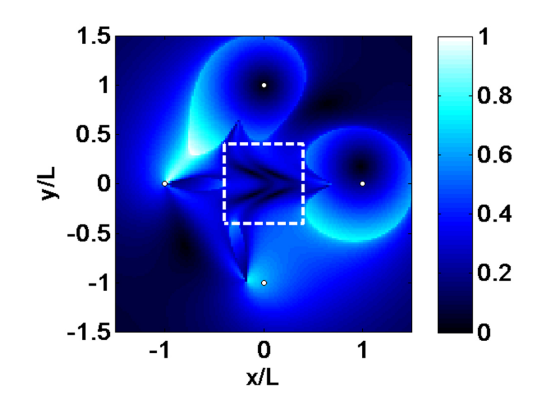


Figure 2. Displacement (dimensionless) during one cycle of the sequence of extractions and injections for each initial position. These results are also shown in Figure S1 of the auxiliary material, along with equivalent results for two, three, and four cycles. Wells are shown as white dots, and the white dashed square is the area shown in Figure 3.

¹Auxiliary materials are available in the HTML. doi:10.1029/2011WR011567.

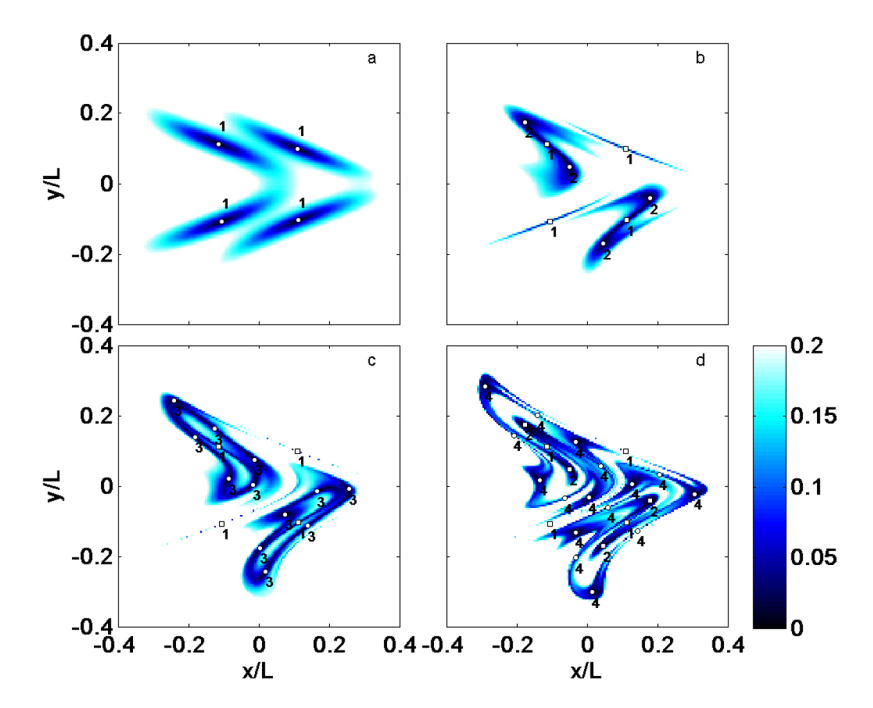


Figure 3. Displacement (dimensionless) during n cycles of the sequence of extractions and injections for each initial position in the dashed white square shown in Figure 2, where (a) n = 1, (b) n = 2, (c) n = 3, and (d) n = 4. In each plot, period n periodic points are shown as white circles, and lower periodic points are shown as white squares. For example, period 1 periodic points appear at each cycle and are shown as white circles in Figure 3a and as white squares in Figures 3b–3d.

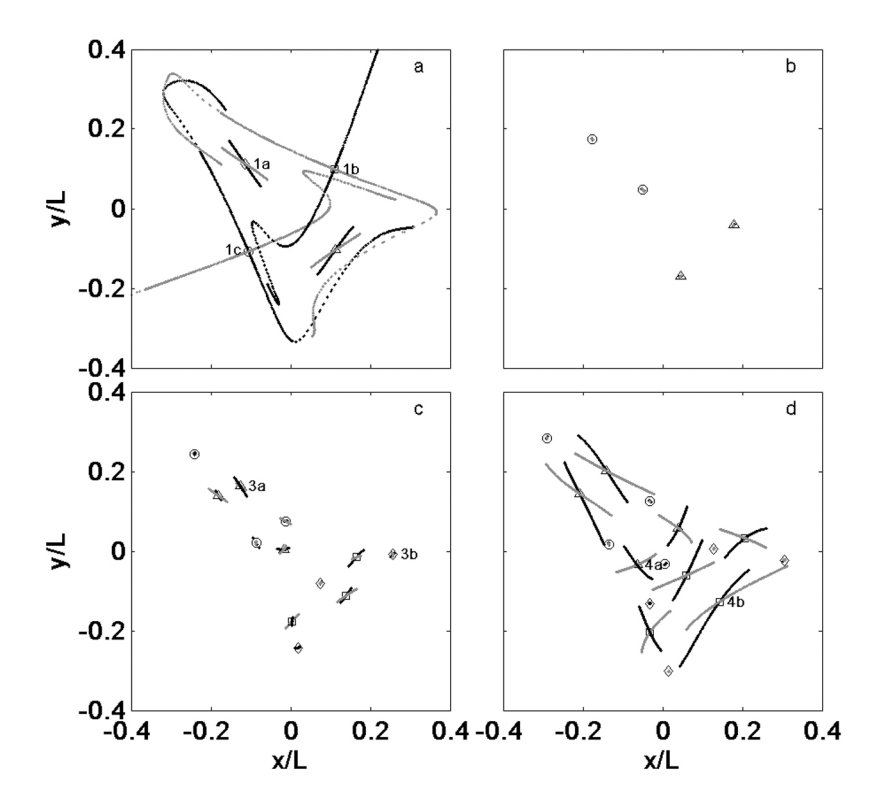


Figure 4. Period n periodic points for the sequence of extractions and injections with stable (gray) and unstable (black) manifolds, where (a) n = 1, (b) n = 2, (c) n = 3, and (d) n = 4. To allow comparisons of magnitude for manifolds associated with different periods, each plot shows manifolds after four iterations of the sequence of extractions and injections. Several heteroclinic points are evident in Figure 4a, indicating the presence of deterministic chaos. In each plot, sets of periodic points are indicated by common plotting symbols. Numbered periodic points are referenced in Figure 5.

remains in approximately the same position throughout the simulation, and thus no manifolds are observed in Figure 4b. These points represent locations where spreading is poor.

- [24] The remaining periodic points are hyperbolic, representing regions of good spreading. The relative degree of spreading can be measured by the lengths of the segments of the manifold that are shown in Figure 4. The segments do not represent the complete manifold, but rather the portion of the manifolds generated in 4 cycles of forward or reverse time. The period 3 periodic points have the least amount of spreading on the basis of the short length of the manifold segments. On the other hand, for two of the period 1 periodic points, labeled 1b and 1c on Figure 4a, the segments of the manifolds are long, indicating a high degree of spreading in the vicinity of these periodic points. For these two periodic points, the stable manifold of one periodic point intersects the unstable manifold of the other; these points of intersection are heteroclinic points, which imply the presence of chaos in this system. If the particle positions were tracked for more than 4 cycles, additional heteroclinic points would be seen in Figure 4a, and new heteroclinic points would emerge in Figures 4c and 4d.
- [25] One can grasp the crucial role of hyperbolic periodic points by recalling that the basic idea of chaos is sensitive dependence on initial conditions. Consider two fluid particles that are initially close to each other, but (just) on opposite sides of a stable manifold of a hyperbolic periodic point. In the first few iterations after they pass the hyperbolic periodic point, these two particles will diverge rapidly. So, by extension, if the domain contains many hyperbolic periodic points, then it will also exhibit good spreading [Funakoshi, 2008; Mosovsky and Meiss, 2011].
- [26] Additional evidence of chaos is seen in Figure 5, which plots $\lambda^{(n)}$ calculated by (2) versus the number of cycles. The selected periodic points are highlighted on Figure 4. The flow exhibits positive $\lambda^{(n)}$, indicating chaotic advection in the first few cycles, similar to the results of the pulsed dipole [Jones and Aref, 1988]. The behavior of the system during the first few cycles is critical for spreading, since the system will be most cost effective if spreading can be achieved in a short amount of time [Swanson and Ottino, 1990].

3.3. Heterogeneity Effects

[27] As discussed in section 1, the discussion to this point has been based on a highly idealized model that

neglects (1) dispersion, in order to focus entirely on spreading, and (2) heterogeneous permeability, in order to focus on heterogeneous velocity resulting from the engineered sequence of injections and extractions. Accounting for dispersion is the subject of ongoing work that will extend this approach to include mixing and remediation reactions. In contrast, heterogeneous permeability (henceforth called heterogeneity) is relevant even when focusing entirely on spreading [Dagan, 1989, section 4.3.5; Kapoor and Gelhar, 1994a, 1994b; Kitanidis, 1994; Le Borgne et al., 2010; Rolle et al., 2009]. Accordingly, this section reports simulations to show the relative contribution of spreading resulting from stretching and folding compared to spreading resulting from aquifer heterogeneity.

[28] Random log hydraulic conductivity fields Y = ln(K)with unit mean hydraulic conductivity and standard deviations $\sigma_Y = 0$, 0.1, 0.3, and 1 were produced from a single realization of sequential Gaussian simulation in GSLIB [Deutsch and Journel, 1992]. Simulations used a spherical variogram with correlation length $I_Y = 2.1L$. As shown in Figure S4 of the auxiliary material, the domain is $\pm 6.005L$ in the x and y directions, chosen to eliminate boundary effects from the assumed constant head condition on each boundary. For each level of heterogeneity, MODFLOW 2000 [Harbaugh et al., 2000] was used to simulate the flow resulting from the 12-step sequence of injections and extractions given in Table 1, assuming specific storage $S_s = 0.001/L$. The plume interface was modeled by particle tracking using MODPATH 5.0 [Pollock, 1994], with porosity $\varepsilon = 0.25$, and particles inserted when necessary to keep the maximum separation distance between adjacent particles no more than 0.0031L [Schafer-Perini and Wilson, 1991].

[29] Results show that spreading by stretching and folding is complimentary to spreading resulting from aquifer heterogeneity. For the homogeneous case of $\sigma_Y = 0$, Figure 6a confirms that the numerical model is consistent with the analytical model of section 3.1, with plume interface lengths of 3.65L and 3.77L for the numerical and analytical models, respectively. Figure 6b ($\sigma_Y = 0.1$) shows minor deviations from the homogeneous case, giving an increased plume interface length of 4.76L, but no apparent extraction of the plume interface. Figure 6c ($\sigma_Y = 0.3$) and Figure 6d ($\sigma_Y = 1$) show larger deviations from the homogeneous case, giving increased plume interface lengths of 11.7L and 114L, respectively. Taken together, these results show that heterogeneity provides additional spreading, and would therefore be

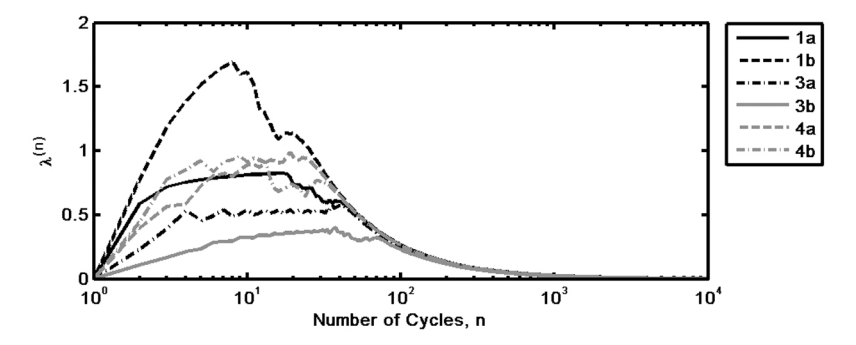


Figure 5. Average values of $\lambda^{(n)}$ for the numbered periodic points shown in Figure 4. Each curve shows the average value of $\lambda^{(n)}$ for 360 particles uniformly spaced around the relevant periodic point on a circle of radius $(1 \times 10^{-12})L$. All curves approach zero asymptotically.

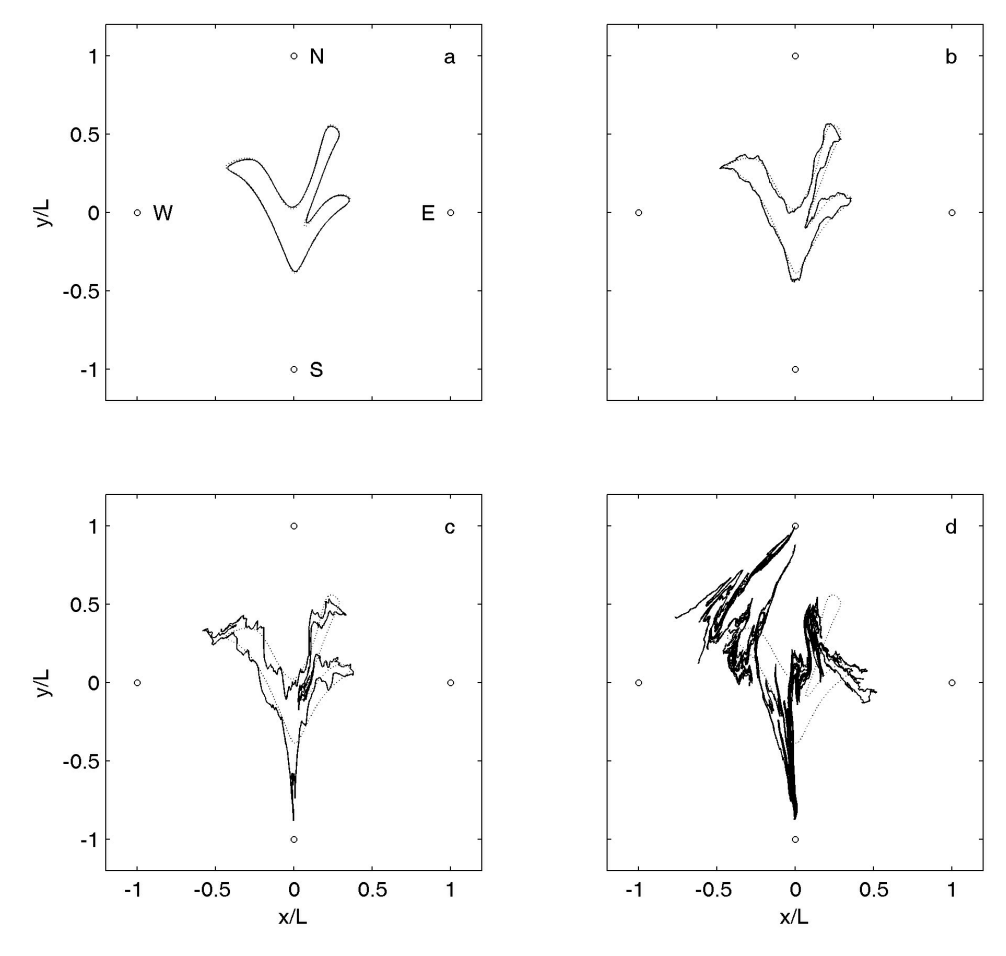


Figure 6. Comparison of plume interface with and without heterogeneity, shown after the 12-step sequence of injections and extractions given in Table 1. The homogeneous case (dotted line) corresponds to Figure 11 and was calculated with the analytical model of section 3.1. The heterogeneous case (solid line) was calculated using the permeability field shown in Figure S4 and the numerical model of section 3.3 for (a) $\sigma_Y = 0$, (b) $\sigma_Y = 0.1$, (c) $\sigma_Y = 0.3$, and (d) $\sigma_Y = 1.0$, where $Y = \ln(K)$ and X is hydraulic conductivity. The open circles are wells at $(0, \pm 1)$ and $(\pm 1, 0)$.

expected to increase mixing of injected treatment solutions. While this is certainly good news for groundwater remediation, Figure 6 also contains an important caveat, because as heterogeneity increases, the plume interface is increasingly likely to be extracted (at well S for $\sigma_Y = 0.3$ and wells N and S for $\sigma_{\rm V} = 1$), which would trigger regulatory and clogging concerns as discussed in section 1. Extraction of the plume interface is not surprising, because the 12-step process in Table 1 was specifically developed for the homogeneous case. In particular, the long plume interface length of 114L for $\sigma_Y = 1$ results not only from heterogeneity, but also from extraction of the plume interface at wells N and S. Given the heterogeneous nature of essentially all geologic porous media, Figure 6 indicates that stochastic optimization should be considered for practical implementation of the stretching and folding approach proposed here. This is the subject of ongoing work.

3.4. Discussion

[30] The approach presented here for plume spreading by stretching and folding is related to the baker's transformation,

which has been called the best possible mixing device [Chakravarthy and Ottino, 1995; Ottino, 1989, section 5.8; Ottino et al., 1994]. However, because it requires cutting and fusing, the baker's transformation cannot be applied directly to continuous flows; its continuous analog, the horseshoe map, is the best available approximation [Ottino, 1989, section 5.8]. The presence of heteroclinic points generally implies the flow is equivalent to a horseshoe map [Ottino, 1989, section 5.9], which means that the engineered sequence of extractions and injections presented here is an example of the larger class of horseshoe maps that is known to be optimal for spreading.

[31] With in situ remediation, improved spreading of the treatment solution will allow increased interactions between the treatment solution and the contaminated groundwater, thereby increasing the potential for contaminant degradation reactions to occur. The presence of hyperbolic periodic points, heteroclinic points, and positive early time Lyapunov exponents indicates that the proposed flow produces chaotic advection, and therefore good spreading. In particular, (1) the extraction-injection sequence can be designed so that the

fluid interface is not extracted, at least in the first few iterations where spreading is crucial, thereby minimizing the risk of clogging and regulatory concerns, and (2) plume spreading is not dependent on background flow. In other words, the scheme proposed here provides an alternative for cases where the background flow is too slow to produce plume spreading on a practical time scale.

[32] Unbounded spreading in an in situ remediation system is not desirable because the contaminant would be spread into regions of the aquifer that were initially uncontaminated. Instead, the goal is spreading at early times, when the injected plume of treatment solution is spread throughout the contaminated region, while still containing the contaminant to a finite region of the aquifer. Such a system would be represented by exponential growth of separation distances for early times when the initial spreading occurs within the finite region, followed by no growth in separation distances at later times because all particles remain in the finite region. The system presented in this paper shows this behavior, as demonstrated by the positive value of the finite time Lyapunov exponent, $\lambda^{(n)}$, at early time, and a value of zero as time increases (Figure 5).

[33] There is remarkable similarity between the unstable manifolds of the hyperbolic periodic points and the geometry of the fluid interface itself. For example, Figure 7 shows the segment of the unstable manifold for period 1 points generated with 7 cycles along with the fluid interface after 4 cycles; Figure S5 in the auxiliary material shows similar results for period 2, 3, and 4 periodic points; and Animation S2 of the auxiliary material shows the correspondence between the plume evolution and one of the unstable manifolds for a period 1 periodic point. Unstable manifolds are infinitely long and have an infinite number of bends of approximately 180 degrees (see Figure 7) where the manifold reverses direction, producing long and narrow filaments. In the context of in situ remediation, as the fluid interface stretches along the unstable manifolds, the fluid interface will also be characterized by these same long and narrow filaments. As these filaments become narrower, their width will approach the length scale for pore-scale diffusion.

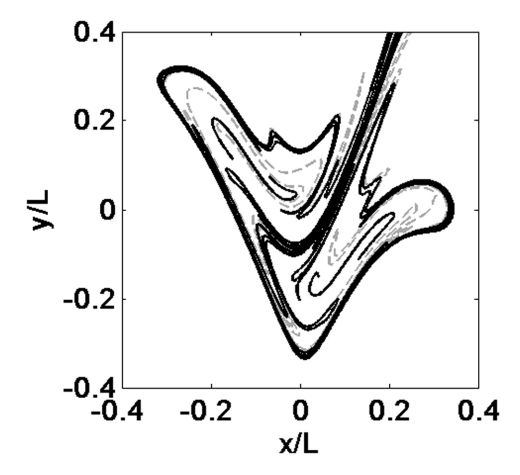


Figure 7. Comparison of the unstable manifold for period 1 points after seven cycles (solid black line) with the fluid interface after four cycles (gray dashed line).

Thus, the longer fluid interface provides more area for reaction while the narrow filaments enable the final pore-scale diffusion step required for mixing and therefore for reaction.

[34] The region of good spreading is determined by the structure of the flow, which can be visualized by the 4-cycle displacement in Figure 3d, by the stable and unstable manifolds in Figure 4a, or by the fluid interface in Figure 7. The correspondence between the region of good spreading and the initial size of the r=L/4 plume is by design, because the 12-step sequence of injections and extractions given in Table 1 was specifically designed for a plume of that size and geometry in a homogeneous aquifer.

4. Conclusions

[35] With in situ remediation, degradation reactions occur where the treatment solution and the contaminated groundwater contact each other, or more precisely, are close enough to interact by pore-scale dispersion on a practical time scale. Spreading promotes mixing, and the fluid mechanics literature indicates that spreading is produced efficiently by chaotic advection. A review of the pulsed dipole shows that it produces chaotic advection, but that it suffers from theoretical and practical limitations. Accordingly, the goal of this paper was to introduce a new conceptual model for chaotic advection to create stretching and folding in order to enhance in situ groundwater remediation. The engineered sequence of extractions and injections introduced in this paper creates a periodic, unsteady flow field in the vicinity of the interface between the treatment solution and the contaminated groundwater, leading to stretching and folding of the fluid interface, which increases contact between the treatment solution and the contaminated groundwater, which will enhance mixing and therefore contaminant degradation. Chaotic advection has been shown to lead to good spreading [Aref, 1984; Ottino, 1989]; thus by demonstrating that the sequence of extractions and injections produces chaotic advection, evidenced by heteroclinic points on the Poincaré section and nonzero Lyapunov exponents at early time, this paper has demonstrated that the engineered sequence of extractions and injections produces good spreading. Moreover, the proposed scheme does not require reiniection, which reduces the risk of clogging and regulatory concerns resulting from extraction of contaminated groundwater, and the proposed scheme does not rely on background flow to produce plume spreading.

[36] The specific sequence of extractions and injections presented in this paper was chosen simply as an illustration to produce stretching and folding, but was not optimized. Moreover, pore-scale dispersion has been neglected. The relative contribution to overall mixing (and enhanced reaction) of the flow proposed here versus pore-scale dispersion is the subject of ongoing work. Aided by plume spreading by stretching and folding, and by the complimentary spreading caused by heterogeneous permeability, improved mixing would be expected to increase reaction rates and consequently the effectiveness of in situ groundwater remediation.

[37] **Acknowledgments.** The authors thank Cristyn Radabaugh, Massoud Asadi-Zeydabadi, Elizabeth Bradley, James Meiss, and Brock Mosovsky for their enlightening conversations on this topic and the three anonymous referees for their insightful and constructive feedback. This work was supported in part by the Hydrologic Sciences Program of the National Science Foundation (EAR-1113996).

References

- Aref, H. (1984), Stirring by chaotic advection, *J. Fluid Mech.*, 143, 1–21.

 Aref, H. (2002). The development of chaotic advection. *Phys. Fluid*.
- Aref, H. (2002), The development of chaotic advection, *Phys. Fluids*, 14(4), 1315–1325.
- Bagtzoglou, A. C., and P. M. Oates (2007), Chaotic advection and enhanced groundwater remediation, *J. Mater. Civil Eng.*, 19(1), 75–83.
- Chakravarthy, V. S., and J. M. Ottino (1995), Mixing studies using horseshoes, Int. J. Bifurcation Chaos, 5(2), 519–530.
- Cirpka, O. A. (2005), Effects of sorption on transverse mixing in transient flows, *J. Contam. Hydrol.*, 78(3), 207–229.
- Cirpka, O. A., F. P. J. de Barros, G. Chiogna, M. Rolle, and W. Nowak (2011), Stochastic flux-related analysis of transverse mixing in two-dimensional heterogeneous porous media, *Water Resour. Res.*, 47, W06515, doi:10.1029/ 2010WR010279.
- Crimaldi, J. P., J. R. Cadwell, and J. B. Weiss (2008), Reaction enhancement of isolated scalars by vortex stirring, *Phys. Fluids*, 20(7), 073605, doi:10.1063/1.2963139.
- Dagan, G. (1989), Flow and Transport in Porous Formations, Springer, Berlin.
- Dentz, M., and J. Carrera (2005), Effective solute transport in temporally fluctuating flow through heterogeneous media, *Water Resour. Res.*, 41, W08414, doi:10.1029/2004WR003571.
- Dentz, M., T. Le Borgne, A. Englert, and B. Bijeljic (2011), Mixing, spreading and reaction in heterogeneous media: A brief review, *J. Contam. Hydrol.*, 120–121, 1–17.
- Deutsch, C., and A. Journel (1992), GSLIB: Geostatistical Software Library and User's Guide, Oxford Univ. Press, New York.
- Domenico, P., and F. Schwartz (1998), *Physical and Chemical Hydrogeology*, 2nd ed., John Wiley, New York.
- Finn, M. D., S. M. Cox, and H. M. Byrne (2004), Mixing measures for a two-dimensional chaotic Stokes flow, *J. Eng. Math.*, 48(2), 129–155.
- Funakoshi, M. (2008), Chaotic mixing and mixing efficiency in a short time, *Fluid Dyn. Res.*, 40(1), 1–33.
- Harbaugh, A., É. Banta, M. Hill, and M. McDonald (2000), MODFLOW-2000, the U.S. Geological Survey modular ground-water model: User guide to modularization concepts and the ground-water flow process, U.S. Geol. Surv. Open File Rep., 00-92.
- Jones, S. W., and H. Aref (1988), Chaotic advection in pulsed source sink systems, *Phys. Fluids*, 31(3), 469–485.
- Kapoor, V., and L. W. Gelhar (1994a), Transport in three-dimensionally heterogeneous aquifers: 1. Dynamics of concentration fluctuations, *Water Resour. Res.*, 30(6), 1775–1788.
- Kapoor, V., and L. W. Gelhar (1994b), Transport in three-dimensionally heterogeneous aquifers: 2. Predictions and observations of concentration fluctuations, *Water Resour. Res.*, 30(6), 1789–1801.
- Kitanidis, P. K. (1994), The concept of the dilution index, Water Resour. Res., 30(7), 2011–2026.
- Kleinfelter, N., M. Moroni, and J. H. Cushman (2005), Application of the finite-size Lyapunov exponent to particle tracking velocimetry in fluid mechanics experiments, *Phys. Rev. E*, 72(5), 056306, doi:10.1103/PhysRevE.72.056306.
- Le Borgne, T., M. Dentz, D. Bolster, J. Carrera, J. R. de Dreuzy, and P. Davy (2010), Non-Fickian mixing: Temporal evolution of the scalar dissipation rate in heterogeneous porous media, *Adv. Water Resour.*, 33(12), 1468–1475.
- Li, L., C. I. Steefel, K. H. Williams, M. J. Wilkins, and S. S. Hubbard (2009), Mineral transformation and biomass accumulation associated with uranium bioremediation at Rifle, Colorado, *Environ. Sci. Technol.*, 43(14), 5429–5435.
- Li, L., C. I. Steefel, M. B. Kowalsky, A. Englert, and S. S. Hubbard (2010), Effects of physical and geochemical heterogeneities on mineral transformation and biomass accumulation during biostimulation experiments at Rifle, Colorado, *J. Contam. Hydrol.*, 112(1-4), 45–63.

- MacDonald, T. R., and P. K. Kitanidis (1993), Modeling the free-surface of an unconfined aquifer near a recirculation well, *Ground Water*, 31(5), 774–780.
- MacDonald, T. R., P. K. Kitanidis, P. L. McCarty, and P. V. Roberts (1999), Mass-transfer limitations for macroscale bioremediation modeling and implications on aquifer clogging, *Ground Water*, 37(4), 523–531.
- Mosovsky, B. A., and J. D. Meiss (2011), Transport in transitory dynamical systems, *SIAM J. Appl. Dyn. Syst.*, 10(1), 35–65.
- Muzzio, F., P. Swanson, and J. Ottino (1992), Mixing distributions produced by multiplicative stretching in chaotic flows, *Int. J. Bifurcation Chaos*, 2(1), 37–50.
- National Research Council (2000), Natural Attenuation for Groundwater Remediation, Natl. Acad. Press, Washington, D. C.
- National Research Council (2009), Advice on the Department of Energy's Cleanup Technology Roadmap: Gaps and Bridges, Natl. Acad. Press, Washington, D. C.
- Ottino, J. M. (1989), The Kinematics of Mixing: Stretching, Chaos, and Transport, Cambridge Univ. Press, Cambridge, U. K.
- Ottino, J. M., S. C. Jana, and V. S. Chakravarthy (1994), From Reynolds stretching and folding to mixing studies using horseshoe maps, *Phys. Fluids*, 6(2), 685–699.
- Pollock, D. (1994), A particle tracking post-processing package for MOD-FLOW, the U.S. Geological Survey finite-difference ground-water flow model: User's guide for MODPATH/MODPATH-PLOT, version 3, *U.S. Geol. Surv. Open File Rep.*, 94-464.
- Pope, S. (2000), Turbulent Flows, Cambridge Univ. Press, New York.
- Radabaugh, C. R. (2011), Groundwater mixing using pulsed dipole injection/ extraction wells, MS thesis, Dep. of Civ. Eng., Univ. of Colo. Denver, Denver, Colo.
- Reynolds, O. (1894), Study of fluid motion by means of coloured bands, *Nature*, 50(1285), 161–164.
- Rolle, M., C. Eberhardt, G. Chiogna, O. A. Cirpka, and P. Grathwohl (2009), Enhancement of dilution and transverse reactive mixing in porous media: Experiments and model-based interpretation, *J. Contam. Hydrol.*, 110(3–4), 130–142.
- Schafer-Perini, A., and J. Wilson (1991), Efficient and accurate front tracking for two-dimensional groundwater-flow models, *Water Resour. Res.*, 27(7), 1471-1485.
- Sposito, G. (2006), Chaotic solute advection by unsteady groundwater flow, *Water Resour. Res.*, 42, W06D03, doi:10.1029/2005WR004518.
- Stefanski, K., K. Buszko, and K. Piecyk (2010), Transient chaos measurements using finite-time Lyapunov exponents, *Chaos*, 20(3), 033117, doi:10.1063/1.3483877.
- Stremler, M. A., F. R. Haselton, and H. Aref (2004), Designing for chaos: Applications of chaotic advection at the microscale, *Philos. Trans. R. Soc. A*, 362(1818), 1019–1036.
- Swanson, P. D., and J. M. Ottino (1990), A comparative computational and experimental-study of chaotic mixing of viscous fluids, *J. Fluid Mech.*, 213, 227–249.
- Tabor, M. (1989), Chaos and Integrability in Nonlinear Dynamics, John Wiley, New York.
- Tel, T., G. Karolyi, A. Pentek, I. Scheuring, Z. Toroczkai, C. Grebogi, and J. Kadtke (2000), Chaotic advection, diffusion, and reactions in open flows, *Chaos*, 10(1), 89–98.
- Trefry, M., D. Lester, G. Metcalfe, A. Ord, and K. Regenauer-Lieb (2012), Toward enhanced subsurface intervention methods using chaotic advection, J. Contam. Hydrol., 127(1-4), 15-29.
- Weeks, S. W., and G. Sposito (1998), Mixing and stretching efficiency in steady and unsteady groundwater flows, *Water Resour. Res.*, 34(12), 3315–3322.
- Zhang, P. F., S. L. DeVries, A. Dathe, and A. C. Bagtzoglou (2009), Enhanced mixing and plume containment in porous media under timedependent oscillatory flow, *Environ. Sci. Technol.*, 43(16), 6283–6288.